NPL
National Physical Laboratory

NPL REPORT IR 33

Characterising the Neutron and Gamma Responses of the NPL Liquid Scintillation Spectrometers

Hawkes, N P

AUGUST 2014

National
Measurement
System

Characterising the Neutron and Gamma Responses of the NPL Liquid Scintillation Spectrometers

Hawkes, N P
Acoustics & Ionising Radiation Division, Operations Directorate

ABSTRACT

Neutron and gamma responses for the smaller of NPL's two liquid scintillation spectrometers were calculated using the programs NRESP7 and PHRESP. The light output and resolution functions required for these calculations were derived from measurements made earlier at various energies in the ranges 1.2 - 15 MeV for neutrons and 0.28 - 1.8 MeV for gammas, together with additional measurements of the proton light output function between 0.9 and 6.4 MeV. Response matrices for this detector were then generated using responses calculated at closely spaced energies. Finally, pulse height spectra from both spectrometers were unfolded to derive energy spectra in cases where the true energy spectra were known, and the results assessed.

ISSN 1754-2952

National Physical Laboratory
Hampton Road, Teddington, Middlesex, TW11 0LW, UK

Approved on behalf of NPLML by Giuseppe Schettino, Knowledge Leader, Acoustics & Ionising Radiation Division.

CONTENTS

FIGURES

TABLES

1 INTRODUCTION

The work described in this Report is a continuation of work reported in a previous NPL publication[1]. The purpose of the project was described there, but is set out again here for completeness.

Neutron spectrometry is important in dosimetry because the quality factor for neutrons changes rapidly with energy in the region from about 10 keV to a few tens of MeV, so the energy spectrum needs to be known in order to convert fluence into dose.

The organic liquid scintillator NE213, or the equivalent BC501A[2], is a popular choice for neutron spectrometry in the part of this region above about 1 MeV because of its high efficiency and its capacity for high count rates. The scintillator is sensitive to gammas as well as neutrons, but it has the property that the two types of radiation generate scintillations with slightly different time profiles, allowing them to be distinguished by pulse shape discrimination (PSD) implemented by suitable electronics.

In 1991, NPL acquired a pair of NE213 neutron spectrometers designed, built and characterised by Green *et al.*[3]. The larger one (referred to as the 'Large' spectrometer) had a scintillator volume 60 mm diameter by 60 mm long, while the 'Small' spectrometer was 20 mm by 20 mm. The scintillator cells were constructed to an in-house design in which the expansion bubble in the scintillator cell (a necessary feature with NE213 because of its high thermal expansion coefficient) was confined to a chamber at the end of the cell furthest from the photomultiplier.

PSD was achieved by the Owen technique[4], in which the last dynode of the photomultiplier is deliberately driven into space charge saturation. The duration of this saturation, and hence the amplitude of the pulse from the dynode, depends on the original pulse shape, and is therefore different for neutron and gamma events of the same light output. An earlier dynode provides an undistorted signal proportional to light output. The two signals are captured in coincidence by a two-parameter data acquisition system, and the neutron and gamma events form two distinct ridges in the parameter space (Figure 1). At NPL the 2-parameter display is conventionally set up with 'Shape' on the Y-axis and 'Energy' (properly 'Light output') on the X-axis. The Owen technique has the advantage that the PSD is done by the photomultiplier's own dynodes, and no specialised shape-sensitive electronics is needed.

Green *et al.* tested and characterised these spectrometers extensively. In particular they provided neutron response matrices to allow the incident neutron spectrum to be unfolded from the measured pulse height spectrum using unfolding codes such as RADAK[5]. These matrices were generated by calculating the detector response at closely spaced energies using the program O5S[6], and then assembling the calculated responses into a matrix in a suitable format for the unfolding program. Green *et al.* validated O5S for this application by measuring the detector response absolutely at several selected neutron energies and then comparing these measurements with the corresponding O5S calculations. The measurements were carried out at the monoenergetic irradiation facilities of NPL, Harwell and Birmingham University.

The spectrometers were incorporated into NPL's suite of instruments and put into routine use. By 2003, however, it had become apparent that their performance was declining. Table 1 shows how the resolution of the 1062 keV Compton edge from ^{22}Na had broadened with time.

Table 1. Variation of ^{22}Na resolution with time.

Detector	Original value (c. 1990)	2003 value	Value with new cell
Large NE213	12 %	24 %	13 %
Small NE213	9½ %	16 %	10½ %

The figures are calculated from the formula

$$\text{Resolution (\%)} = \frac{100\,(C_{12.5} - C_{87.5})}{C_{50}} \qquad (1)$$

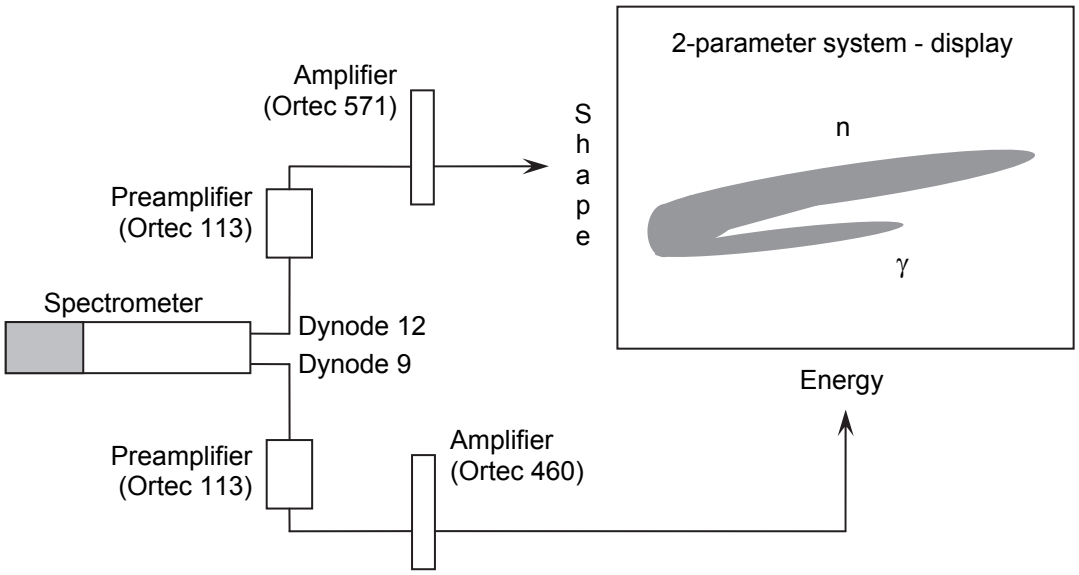

Figure 1. Data acquisition system used with the NPL NE213 spectrometers (schematic).

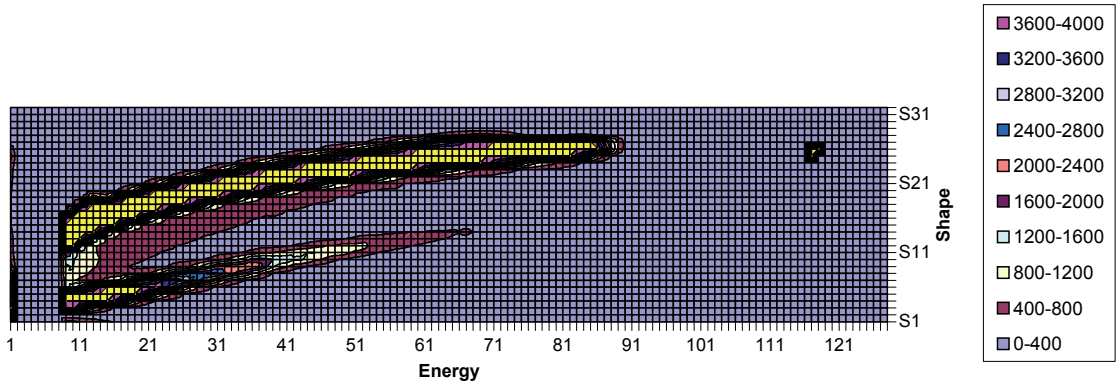

Figure 2. A typical actual 2-parameter histogram corresponding to the above schematic. (The bright yellow colouration denotes cells with more than 4000 counts.)

where C_p is the spectrum channel number (counting from the channel that corresponds to zero light output) at which the counts-per-channel figure is p% of the maximum at the edge.

Inspection of the scintillator cells raised suspicions about the condition of the scintillator. NE213 is normally a clear liquid (with perhaps a hint of blue under some lighting conditions), but the liquid in the cells was pale green. Furthermore, a large number of blister-like raised areas could be seen in the reflective paint on the inner surface of the cells. These effects are not known to be problems with NE213[7], even in cells as old as those here, and they remain unexplained. Nevertheless, the scintillator was clearly implicated, and the decision was taken to replace the cells with new ones of the same size and shape containing BC501A.

The cell design chosen was the MAB-1 type[2], in which the expansion bubble is confined to a coiled tube within the hollow curved side wall of the cylindrical chamber. The casings of the original spectrometers were modified to allow the new cells to be attached, but no other alterations were made. In particular, the Owen PSD system was retained. The new cell design meant that the favoured orientation for irradiations was now end-on instead of side-on as previously.

When the ^{22}Na resolutions were re-measured, the results were as shown in the final column of Table 1. The new resolution figures were greatly improved, being nearly restored to the 1990 values, and the scintillator replacement was deemed successful. However, with such a large change to the spectrometers, it was felt necessary to re-characterise them.

Such work requires significant effort, as detailed in this report, but also afforded the opportunity to update the neutron response matrices using the more modern programs now available for calculating neutron responses. Furthermore, with the availability of similar programs for gammas, additional matrices could be produced to allow gamma spectra to be unfolded. The original aim had been to derive neutron and gamma spectra simultaneously by placing a dividing line between the two ridges of Figure 2 and processing both sets of data. Unfortunately, one cannot always be confident that the PSD system leaves the gamma pulse height spectrum undistorted (as explained in Ref. 1), so there is less potential in this idea than expected. However, gamma response matrices will still be valuable in cases where no neutrons are present or if the problem with the PSD system is overcome.

2 SCOPE OF THE PRESENT WORK

The aim of the present work was to complete the production of new neutron response matrices, and of gamma matrices for the first time, for the NPL liquid scintillation spectrometers. The first part of the project was documented in Ref. 1.

Response matrices are usually generated by calculation, as it is not practical to make monoenergetic response measurements at the large number of closely spaced energies required, and monoenergetic neutrons or gammas may not be available at all the necessary energies. A typical sequence of steps is as follows:

- Absolute measurements (i.e. with precisely known incident fluences) of the spectrometer response are made at selected energies. Additional measurements may be made at other energies.
- The light output of the spectrometer as a function of energy, and its resolution as a function of light output, are deduced.
- These functions are incorporated into the code to be used to calculate the responses. The code is then validated by setting it up to reproduce the geometry of the absolute experiments, and comparing the calculations with the measurements.
- Assuming the comparison is satisfactory, the code is used to calculate a large number of responses spaced closely in energy. A general-purpose geometry (e.g. a parallel incident beam) is used in the absence of more specific information about how the spectrometer will be used.
- The calculated responses are assembled into a response matrix in the format required by the chosen unfolding program.

In the present work, the program used for calculating gamma responses was PHRESP[8], and that for neutron responses was NRESP7[9]. The response matrices were constructed in a format suitable for use with the unfolding code GRAVELW, which is part of the HEPROW[10] package. All these programs originate from the Physikalisch-Technische Bundesanstalt (PTB) in Germany.

Ref. 1 covered the following parts of the work:

- Absolute measurements of the responses of both spectrometers to monoenergetic neutrons and gammas;
- Additional measurements of the proton light output at selected energies;
- Derivation of the electron and proton light output as functions of energy, and of the resolution as a function of light output, for the Large spectrometer;
- Derivation of neutron and gamma response matrices for the Large spectrometer.

This Report describes the following additional work:

- Derivation of the light output and resolution functions for the Small spectrometer;
- Derivation of neutron and gamma response matrices for the Small spectrometer;
- Tests of the effectiveness of gamma and neutron spectrum unfolding, in cases where the true incident spectrum is known.

3 LIGHT OUTPUT UNITS

The light produced by electrons is commonly regarded as linear with energy (with a small offset), provided the energy is above about 40 keV[11]. (Some authors[12] report that the output becomes non-linear again above 1.6 MeV.) Assuming the linear relationship holds, the light output L_e in "light output units" (LU) is therefore related to the electron energy E in MeV by

$$L_e = c\,(E - E_0) \qquad (2)$$

where c is a constant. Reported values of E_0 differ between authors, but are commonly in the region of 0.005 - 0.015 MeV[12, 13]. The PTB convention for light output units, which will be adopted here as well, is to set c = 1 LU / MeV and to define 1 LU as the light produced by an electron of energy (1 + E_0) MeV.

An additional convention adopted in the present work is that the bins in pulse height spectra are labelled with the light output at the centre of the bin.

4 MEASUREMENTS

The experimental method for the gamma and neutron measurements was detailed in Ref. 1. A summary is given here for completeness.

4.1 GAMMA MEASUREMENTS (ABSOLUTE)

Several different gamma-ray sources were used in order to obtain responses over as wide an energy range as possible. The source types are set out in Table 2. Most of the sources were disc-type Isotrak point sources[14], except for ^{24}Na, which has a half-life of only 15 hours and is not available commercially. This source was prepared by the NPL Radioactivity Group, from material activated at the Consort reactor[15] in Ascot, and took the form of an active deposit a few millimetres in diameter on thin plastic film. The activities of the sources (which ranged from approximately 100 - 800 kBq) were calculated from the manufacturer's certificate, or Radioactivity Group data, giving the activity of the particular source at a specified reference date.

Table 2. Gamma ray sources used in the measurement.

Nuclide	Gamma energy, MeV	Compton energy, MeV
^{24}Na	2.754	2.520
"	1.369	1.154
^{88}Y	1.836	1.612
"	0.898	0.699
^{60}Co	1.333	1.118
"	1.173	0.963
^{22}Na	1.275	1.062
"	0.511	0.341
^{54}Mn	0.835	0.639
^{137}Cs	0.662	0.477
^{203}Hg	0.279	0.146

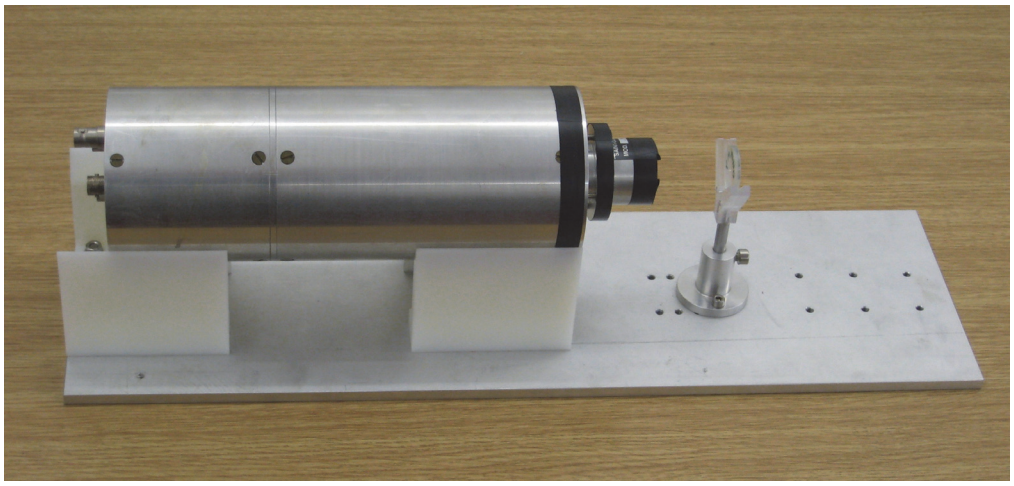

Figure 3. The Small spectrometer, mounted on the jig for gamma source measurements.

The source and spectrometer were mounted on a custom jig (Figure 3), which positioned the source on the spectrometer axis and at a well-determined distance from the front face (4.15 cm for the Small spectrometer). A precision pulser was used to relate the gains of different measurement runs to each other and to establish each run's zero position (the spectrum channel number, non-integral in general, that corresponds to zero light output).

As detailed in Reference 1, it became evident part way through the programme of experimental measurements that the 2-parameter data acquisition mode required for pulse shape discrimination (Figures 1 and 2) could produce some distortion in gamma spectra. Consequently all the gamma spectra except that for ^{24}Na (and some calibration runs) were acquired in a single-parameter mode in which the Energy ADC operates independently and the Shape data are not used. This was possible because discrimination was not required in the absence of a neutron field.

4.2 NEUTRON MEASUREMENTS

4.2.1 Absolute

Measurements were carried out with monoenergetic neutrons at 1.2, 2.5 and 5.0 MeV, produced at the NPL neutron facility. In addition, the spectrometers were taken to PTB for monoenergetic

measurements at 16 and 17 MeV (Large spectrometer) and 15.5 MeV (Small). In each case, the spectrometer was placed in the facility's low-scatter area at a known distance of about 1.5 m from the neutron-producing target. A shadow cone run was carried out at each energy to allow the room scatter component to be subtracted.

Spectra were acquired in the 2-parameter mode described above, and neutron data subsequently extracted using the utility programs that form part of the spectrometry system. Essentially the operator sets up a dividing line on the 2-dimensional data plot, endeavouring to keep all neutron events on one side and all gamma events on the other, and then selects which of the two subsets to save for further processing. A new line is drawn for each new measurement.

At NPL, the neutron fluence delivered to the spectrometer was determined by calibrating the beam monitors (a beam current integrator and a wall-mounted neutron detector) using the NPL long counter. The fluence during the measurement was calculated from the current integrator result (Large spectrometer) or an average of the current integrator and neutron detector results (Small spectrometer, taking advantage of an improvement in the standard analysis technique since the processing of the Large spectrometer data). For the Small spectrometer at 2.5 MeV, the current integrator gave an anomalous result (thought to have been due to an instability in the beam steering), and so the neutron detector result alone was used in this case.

At PTB, the measurements were carried out at the same time as an international comparison of neutron fluence monitors, and therefore PTB could not provide their value for the fluence delivered to the instrument as they normally would. However, the NPL De Pangher long counter was part of the comparison exercise, and so the value from that was used to provide a calibration for the PTB neutron monitor for each day.

4.2.2 Non-absolute

It is desirable to have neutron data at a large number of energies in order to establish the scintillator's light output for protons as a function of proton energy. Absolute measurements, in which the neutron fluence is known, are time consuming, and generally only one neutron energy can be set up and used in a day. However, for determining the light output it is not necessary to know the delivered fluence; all that is needed is the position of the upper edge of the pulse height distribution. Similarly, the room scatter need not be known, as it is expected to affect only the low energy part of the spectrum. A separate set of measurements was therefore carried out at NPL, omitting the long counter calibrations and shadow cone measurements but covering 14 neutron energies from 0.6 to 6.4 MeV in one 8-hour day (once set up).

Neutron / gamma discrimination was required as previously described, and at least one measurement with a ^{22}Na gamma source was made each day in order to establish the energy calibration. The precision pulser was used as before to relate runs at different gains and to establish the channel number corresponding to zero light output.

5 ANALYSIS AND CALCULATION

5.1 GAMMA SPECTRA

5.1.1 Electron light output and spectrometer resolution

Gamma rays striking an organic scintillator do not produce light directly, but (at the energies of interest here) only via the knock-on electrons that they produce in it. The first stage in the calculation of the gamma spectra is therefore to establish the light output function for electrons.

The predominant mechanism by which gammas interact with the electrons in the scintillator is Compton scattering. This produces a spread of electron energies up to a sharp cutoff at the Compton energy E_c, a quantity that is related to the gamma-ray energy E_γ by

$$E_c(E_\gamma) = \frac{E_\gamma}{1 + \dfrac{m_e c^2}{2E_\gamma}} \qquad (3)$$

where $m_e c^2$ is the rest energy of the electron (0.511 MeV). Measurements with suitably selected sources therefore produce a set of relatively sharp Compton edges at the corresponding values of E_c, and by measuring the light output at these edges the relationship between electron energy and light output can be established. (If the form of equation (2) is being assumed, this means finding the value of the E_0 parameter.)

In locating the Compton edges it is convenient to use the half-height, i.e. the position at which the number of counts per channel has fallen to half that at the peak. Unfortunately this does not correspond exactly with the true position of the edge, because of the effect of detector resolution. Figure 4 shows a typical Compton distribution with no added resolution (black curve), and also the same distribution with successively broader Gaussian smearing (coloured curves). The filled circles show the half-height positions of each smeared edge, and it is clear that these positions are increasingly displaced above the true position as the smearing is increased.

As was pointed out by Dietze[16] and by Dietze and Klein[11], the extent of the displacement will depend on the original shape of the unsmeared Compton distribution, i.e. on the gamma ray energy and the size and shape of the scintillator, as well as the extent of the smearing. For a correct calibration, the displacement factor (the ratio of the Compton edge's half-height position to the true Compton position) must be known for each gamma-ray energy and for the particular spectrometer in question.

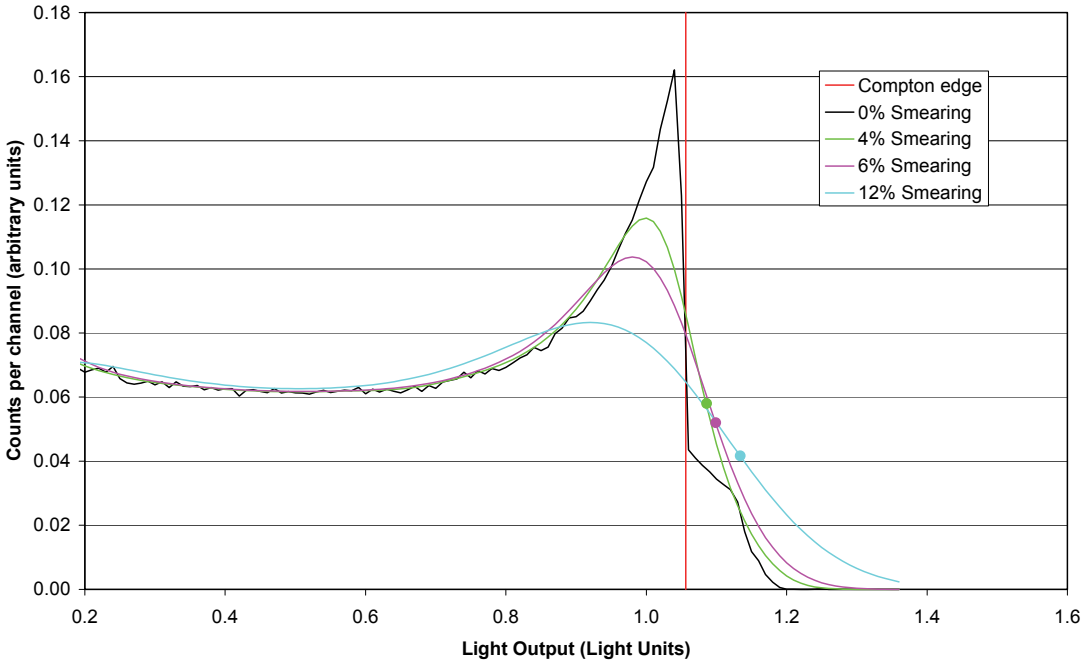

Figure 4. Displacement of the Compton edge half-height with resolution.
The filled circles show the half-height positions for each smeared edge, and the progressive displacement away from the true Compton position is evident. (The shoulder above the sharp edge on the 0% spectrum is due to multiple scattering. The meaning of the smearing percentages is as follows: for each smeared curve, the standard deviation of the Gaussian smearing is fixed, and equal to the stated percentage of the true Compton edge light output.)

For the Small spectrometer, this was done using the following procedure:

(i) An approximate electron light output function $L'_e(E)$ was assumed (by setting E_0 in equation (2) to the value of 0.013 MeV previously found for the Large spectrometer), and incorporated into the program PHRESP.

(ii) PHRESP was used to calculate an unsmeared Compton spectrum for the specific gamma energy being considered, and for the dimensions of the Small spectrometer and the location of the source in the gamma measurement runs.

(iii) The calculated spectrum was overlaid on the corresponding measured spectrum, using an adjustable scaling factor s on the horizontal axis and an adjustable degree of smearing.

(iv) The horizontal scaling and the degree of resolution were adjusted to obtain the best fit to the measured spectrum in the region of the Compton edge.

(v) The Compton edge displacement factor f was then found from the ratio of the observed half-height position h (non-integral in general) and the known "true" position:

$$f = (h - z)s / L'_e(E_c(E_\gamma)) \qquad (4)$$

where z is the zero position for the measured spectrum, s is the fitted horizontal scaling factor in light units per channel, and $L'_e(E)$ is the approximate light output function assumed for electrons in step (i).

(vi) The spectrometer resolution at the Compton edge position was also now known (being just the fitted value of the added resolution).

In step (iii), the applied resolution was of fixed width (specified as a certain percentage of the light output at the true Compton edge), because the variation of resolution with light output was not yet known. This is acceptable because fitting was only carried out over the edge region, which is narrow compared with the full extent of the spectrum.

In step (iv), the calculated spectrum was scaled automatically in the vertical direction so that the total area in the region of the edge matched that of the measured spectrum (see Figure 5). As automatic optimisation is not readily available in Excel spreadsheets, fitting was carried out manually. The resolution was changed in steps of 0.1 percentage points, and the horizontal scaling factor in steps of 1 in the fourth significant digit, until the sum of squared residuals reached a minimum. In the case of ^{60}Co, which has two gamma lines close together in energy, the calculated spectrum was produced by adding together the spectra for the two individual gamma energies in the appropriate proportion. There were therefore three parameters to be adjusted (the resolutions of both gammas and the horizontal scaling), and partial automation of the search process was introduced to make the procedure practical.

Figure 5 gives an example of the process for the case of ^{22}Na.

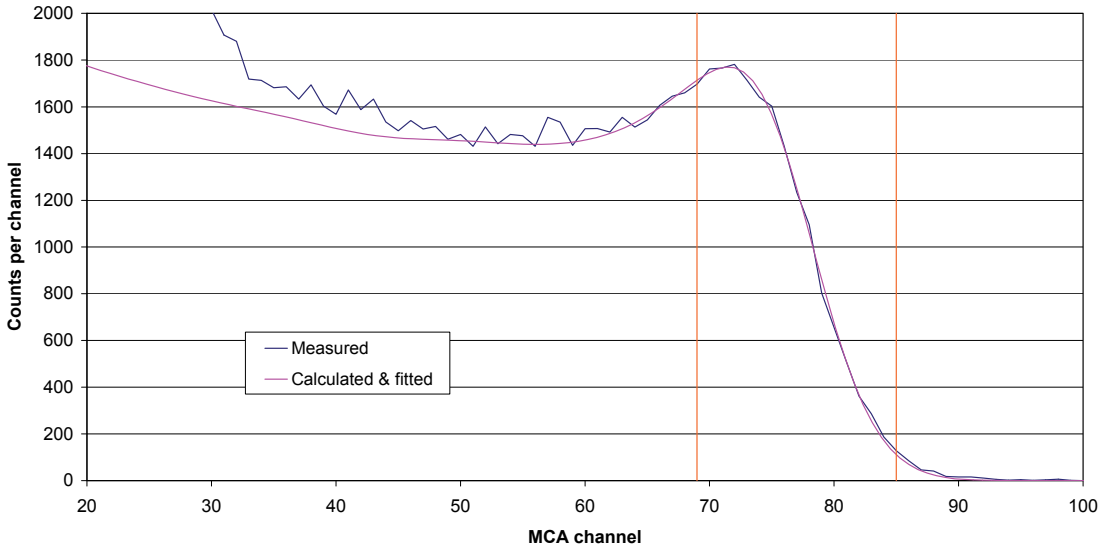

Figure 5. Typical outcome of the Compton edge fitting process.
Fitting is confined to the region between the vertical lines. In the case shown here (^{22}Na), the displacement factor deduced from the fitted spectrum is 1.019 and the standard deviation of the smearing Gaussian is 5.0% of the Compton edge light output.

This process differs from that used previously for the Large spectrometer. The new process has the advantage that the displacement factor and resolution are determined directly for the measured spectrum, but unlike the old process there is no information of wider applicability (e.g. nothing is deduced about the displacement factor at resolutions other than the one seen in this measurement).

Steps (i) – (vi) were repeated for all the gamma sources except ^{24}Na, which was omitted from the calibration process and used as a test of the unfolding procedure instead (see below).

Table 3 shows the displacement factors and resolutions deduced for the Small spectrometer at the calibration energies. Figure 6 shows the electron light calibration resulting from the displacement-corrected edge positions, and Figure 7 shows how the spectrometer resolution varies with light output.

Table 3. Displacement factors and resolutions deduced for the Small spectrometer.

Nuclide	Gamma energy, MeV	Compton energy, MeV	Displace-ment factor	Resolution, FWHM %
^{88}Y	1.836	1.612	1.013	10.1
^{60}Co (high)	1.333	1.119	0.948	12.0
^{22}Na	1.275	1.062	1.019	11.8
^{60}Co (low)	1.173	0.963	1.102	12.5
^{54}Mn	0.835	0.639	1.027	14.8
^{137}Cs	0.662	0.477	1.031	17.0
^{203}Hg	0.279	0.146	1.058	32.3

In Table 3, the displacement factors for ^{60}Co are anomalous because the two close Compton edges merge together in the measured spectrum (Figure 9), and the only calibration quantity that can easily be extracted from the measured spectrum is the half-height position of the combined edge. This is then related to the two component Compton energies by repeating step (v) above for each one, producing two anomalous displacement factors, one larger than usual and the other smaller.

In Figure 6, the straight line (shown dotted) fitted to the displacement-corrected data produces an x intercept of 21.3 keV, indicating that the value of E_0 in equation (2) is 0.0213 MeV for the Small spectrometer. The displacement factors used to obtain this fit were of course derived using the estimated value $E_0 = 0.013$ MeV, but it is assumed that the factors and the resolutions are not sensitive to small changes in the light output function. The horizontal scaling factors s found in step (iv) obviously play no direct part in the light output calibration, as they would simply recover the estimated light function.

The purple circles in Figure 6 show what would happen to the calibration data if the displacement factors were not included. The ^{60}Co data are omitted because the half height of the combined ^{60}Co edge does not obviously correspond to any particular electron energy.

Figure 7 shows the resolution data (expressed as the percentage FWHM of the smearing Gaussian) from Table 3. There are expected[11] to be three different contributions to the resolution, each with a different dependence on the light output L:

- a constant term, from the position-dependent transmission efficiency of light from the scintillator to the photomultiplier;
- a term in $1/L^{0.5}$, due to photon and electron statistics;
- a term in $1/L$, due to electronic noise.

The total resolution will then consist of these three components added in quadrature. On the further expectation[17] that the resolution depends only on the light output, and not on the type of event producing it, the resolution data from the neutron measurements (to be described in Section 5.2.1) have also been included. The program OriginPro[18] was used to fit the assumed function, and the Figure shows that the fit to the combined data is reasonable. The fitted values of the three parameters are shown.

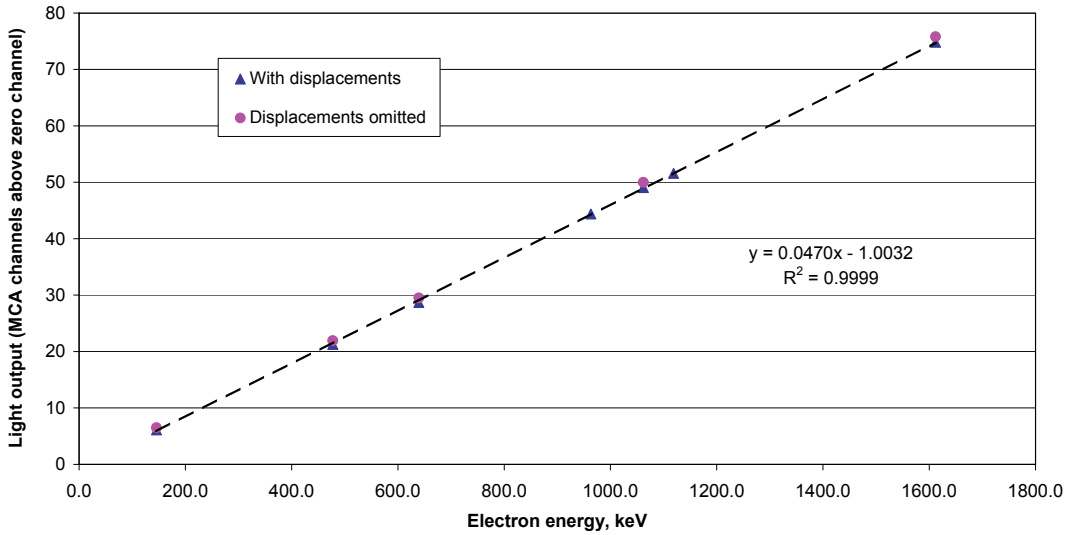

Figure 6. Electron light output calibration for the Small spectrometer.
The equation is that of the trend line (dotted) that is fitted to the blue triangles (data with displacement factors included). The purple circles show the effect of omitting the displacement factors.

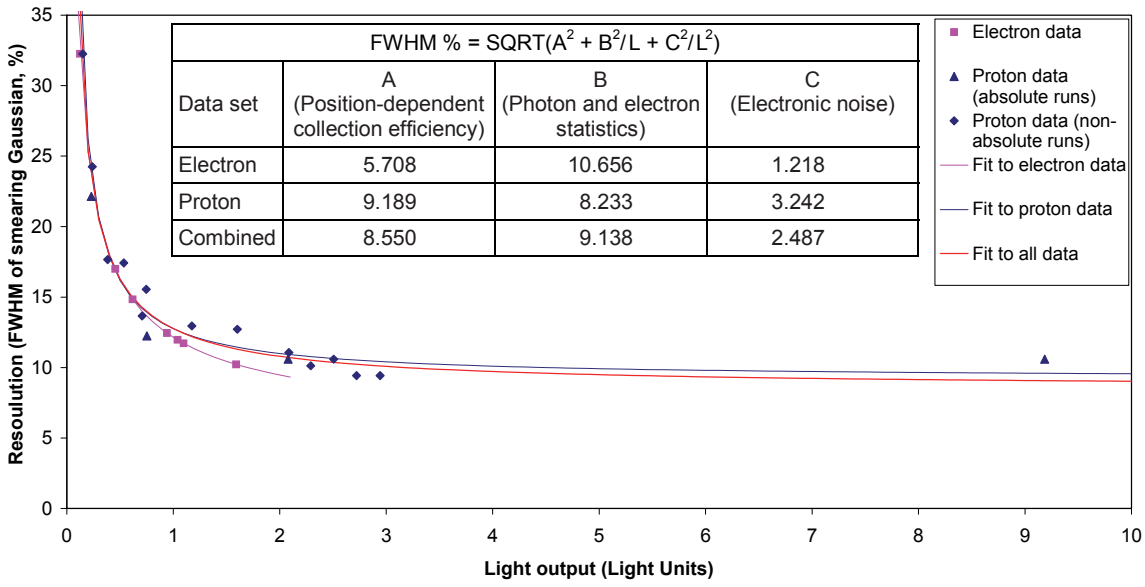

Figure 7. Resolution of the Small spectrometer as a function of light output.
Separate fits are shown for the gamma (electron) data alone, the neutron (proton) data alone, and all data combined. On the assumption that the resolution depends only on the light output, and not the type of event, the fit parameters for the combined data were adopted for the response calculations. Note the resolution is given in terms of (percentage) FWHM rather than standard deviation.

5.1.2 Comparison of calculated and measured gamma spectra

The electron light output function determined above was incorporated into PHRESP, and new spectra calculated for each of the sources. Where the source produces more than one gamma energy, spectra were calculated for each and added in the appropriate proportion, as given in the on-line data[19] provided by the Laboratoire National Henri Becquerel for the Decay Data Evaluation Project. Gaussian smearing was applied with the light-dependent width described by the expression in Figure 7, i.e.

$$\text{FWHM}\ (\%) = (A^2 + B^2/L + C^2/L^2)^{0.5}$$

with A = 8.550, B = 9.138 and C = 2.487.

For the measured spectra, the MCA calibration in terms of light units was established using the upper Compton edge from ^{22}Na as a reference. The number of light units per channel for the ^{22}Na measurement run was set to

$$\frac{f\,L_e(E_c(E_\gamma))}{(h-z)} \qquad (5)$$

where f = 1.019 is the applicable displacement factor (Table 3),
$L_e(E) = E - 0.0213$ is the electron light output formula for the Small spectrometer,
E_γ = 1.275 MeV is the higher gamma energy,
and h and z are the half-height position of the upper edge and the zero position respectively.
The light output calibrations for the other runs then followed via the known relative gains.

PHRESP could now be validated by comparing the calculated and measured spectra for each source. This is shown in Figures 8 - 13 below. In each case, the vertical axis is in counts per unit fluence of the stated gamma ray at the spectrometer face, divided by the bin width in light units. The decay of the source since the reference date on the calibration certificate was included in the calculation, using the half-life values from Reference 19.

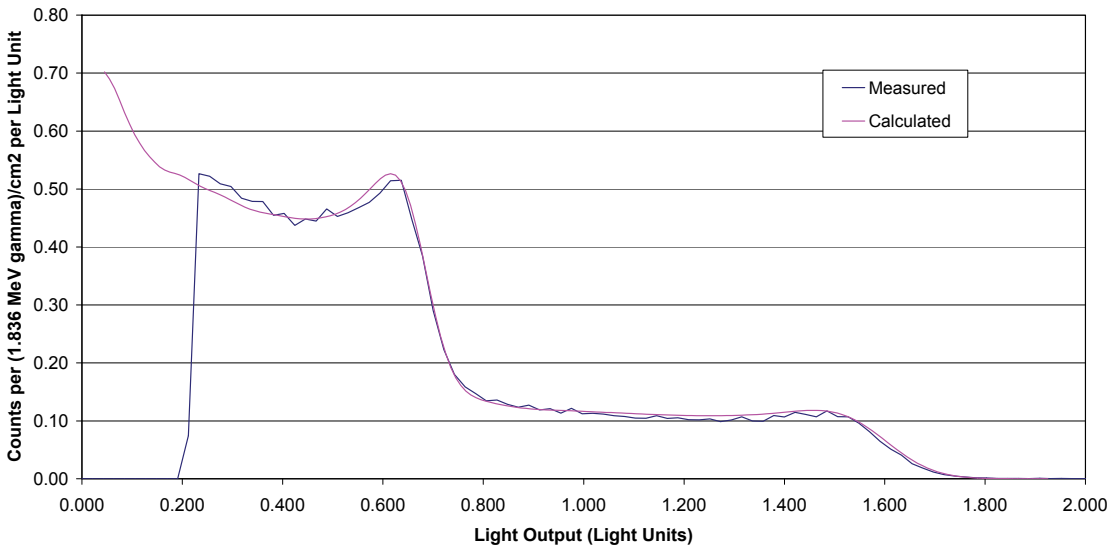

Figure 8. ^{88}Y pulse height spectrum, measured and calculated.

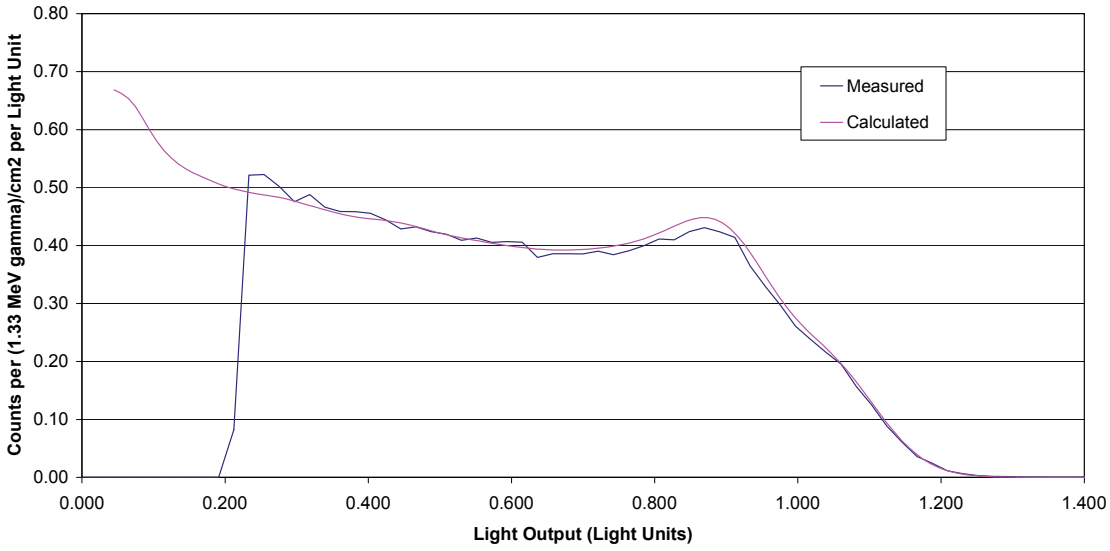

Figure 9. ^{60}Co pulse height spectrum, measured and calculated.
Note the compound Compton edge formed by the merging of two close edges.

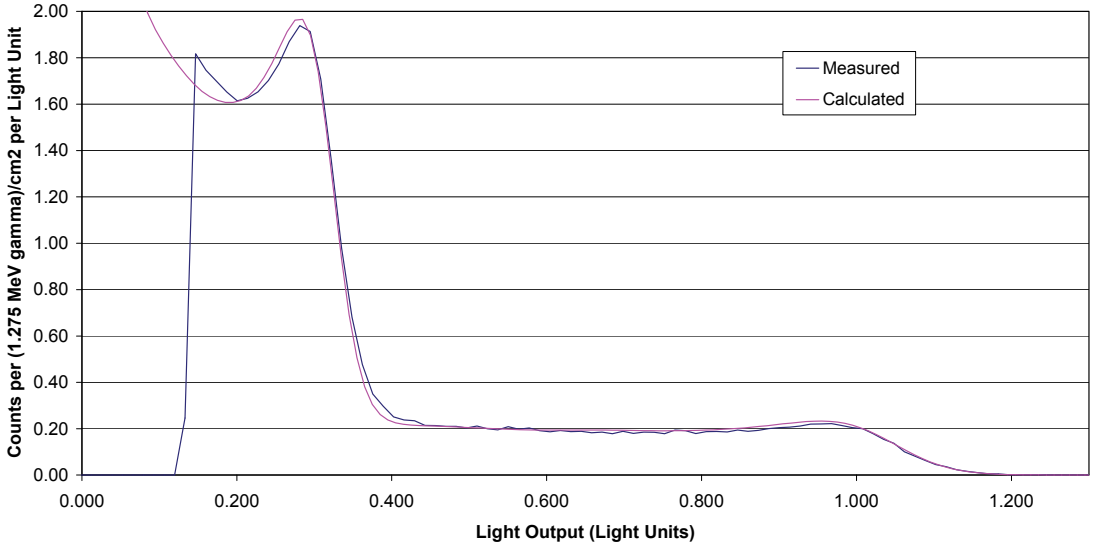

Figure 10. ^{22}Na pulse height spectrum, measured and calculated.

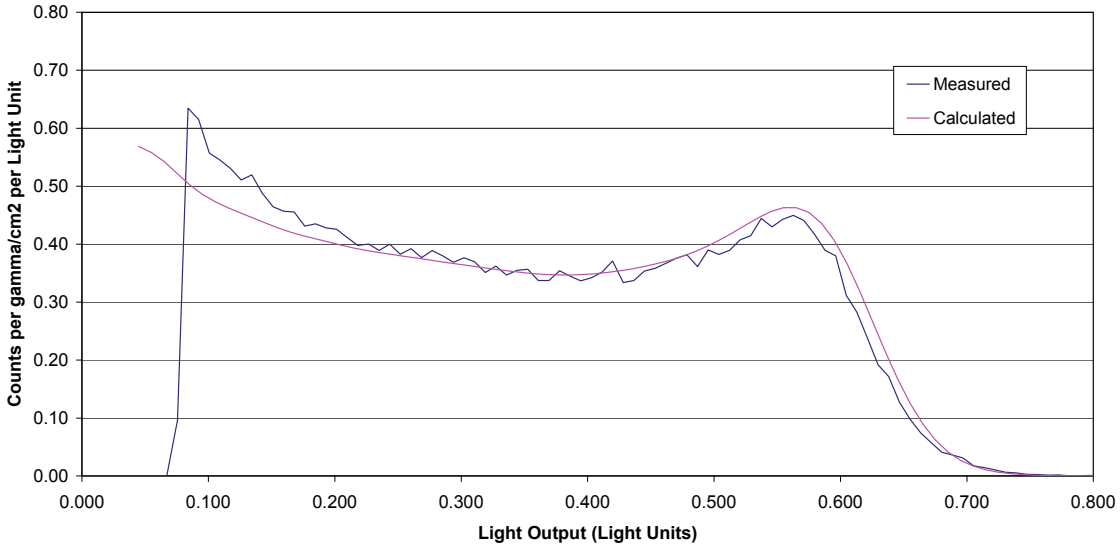

Figure 11. ^{54}Mn pulse height spectrum, measured and calculated.

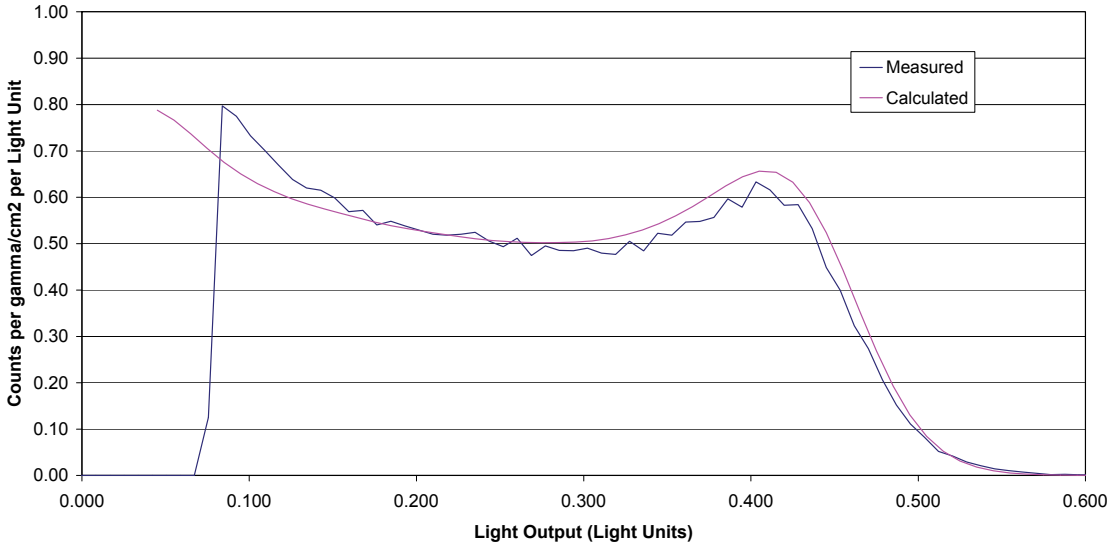

Figure 12. ^{137}Cs pulse height spectrum, measured and calculated.

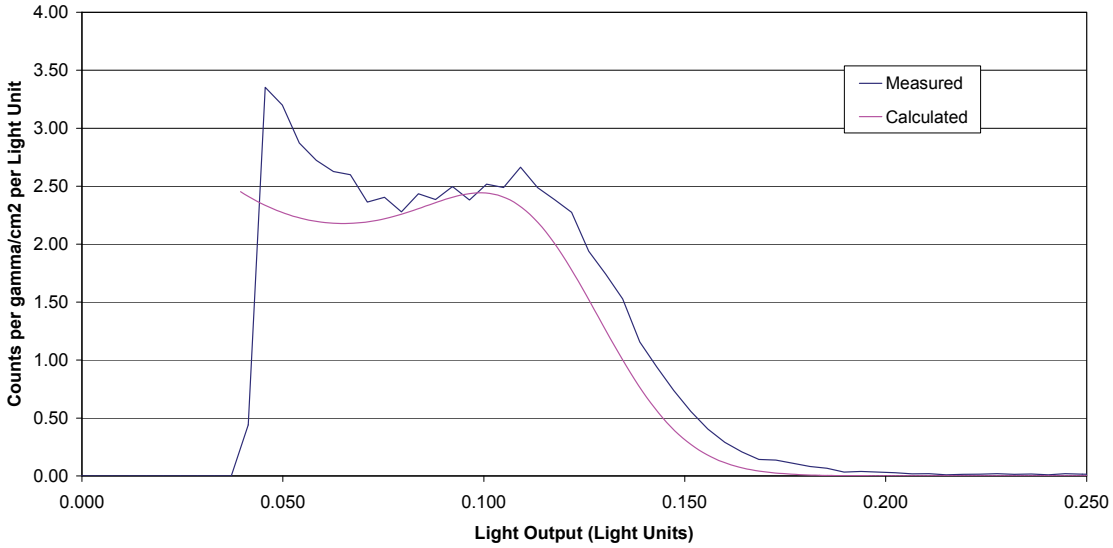

Figure 13. ^{203}Hg pulse height spectrum, measured and calculated.

The vertical scale is absolute in all cases, the activity and distance of the gamma source having been used to derive the amplitude of the measured spectra. For all sources except ^{22}Na, the horizontal scale is also absolute, except in so far as the source contributed to the light output determination. In cases where the source has two distinct gamma lines, only the upper was used in the light output determination, and the lower can be taken as fully absolute.

The match between measurement and calculation is generally reasonable to good, especially at the higher gamma energies. There is a tendency for the calculation to lie above the measured curve at high light outputs, and below it at low, suggesting that some pulses are being subjected to an unexpected degree of attenuation, or that the spectrometer is generating additional low-amplitude pulses. The light output discrepancy in the ^{203}Hg spectrum (Compton energy 146 keV) indicates that the assumed light output formula may diverge slightly from the actual light output at low light values.

PHRESP was considered to have been validated for the Small spectrometer by this exercise, and the construction and use of a gamma response matrix is described in Section 6.1 below.

5.2 NEUTRON SPECTRA

5.2.1 Proton light output

As with the gamma data, the first step is to establish the applicable light output function.

The main interaction mechanism for neutrons striking an organic scintillator is elastic scattering from a proton. For monoenergetic neutrons, and if multiple scattering is neglected, this results in a rectangular distribution of proton energies from zero up to the energy of the neutrons. Hence the upper edge of this recoil distribution corresponds to protons having the same energy as the neutrons.

Factors such as non-linearity of the proton light output and multiple scattering of the neutrons distort the pulse height spectrum away from the basic rectangular shape. However, provided this distortion is not great, there is near symmetry about the upper edge, and the addition of detector resolution effects would not be expected to produce a significant displacement of the apparent edge position (unlike the gamma case). Therefore it is acceptable to take the half-height of the top edge of the spectrum as a good measure of the true recoil edge position, provided care is taken to disregard the multiple scattering component (indicated by a second, diffuse, edge at a lower light output than the single-scatter edge).

However, this approach (which was used in Reference 1 for the Large spectrometer), does not give a value for the spectrometer resolution, which has to be estimated separately using the 7/8 – 1/8 width of the edge. In the present work, software for edge fitting had already been developed for the gamma analysis, so it was decided to follow a procedure similar to the gamma case:

(i) The neutron response program NRESP7 was set up to use an approximate proton light output formula (in fact the formula found previously for the Large spectrometer), and the neutron source distance was set to an arbitrary value representative of the distances used in the measurements. Resolution effects were switched off by a minor edit to the program, so that all results were resolution-free.

(ii) A calculation was carried out for each measured energy, and the result overlaid on the corresponding measured spectrum using adjustable horizontal scaling and resolution.

(iii) The horizontal scaling and resolution were adjusted until a fit to the measured spectrum was obtained in the region of the edge. The resolution width in a given spectrum was held constant with light output (because the nature of the variation was not yet known), but this was acceptable because the edge region is relatively narrow.

(iv) The half-height position of the edge was then determined by inspection of the fitted calculated spectrum. The spectrometer resolution at the light output of the edge was taken as equal to the added resolution.

This procedure has the additional advantage that it is easier to determine a half-height from a smooth curve than directly from an experimental spectrum with random fluctuations. Also, displacement factors f analogous to the gamma case were automatically derived as part of this procedure, but as they were typically very close to 1, the value $f = 1$ was adopted throughout.

Figure 14 shows a typical outcome of the edge-fitting process, in this case for the non-absolute 2.5 MeV measurement. Compared with the gamma case, the absence in the neutron spectra of a peak near the edge made locating the edge more difficult, and it was not always clear where the transition or ‘knee’ from the edge to the nominally flat top of the recoil distribution should be considered to lie. Fortunately the steepness of the edge means that the half-height position is not very sensitive to the assumed location of the knee. In the case of the 0.6 MeV measurement, there was no discernable knee at all, and this measurement was not used in the light output determination.

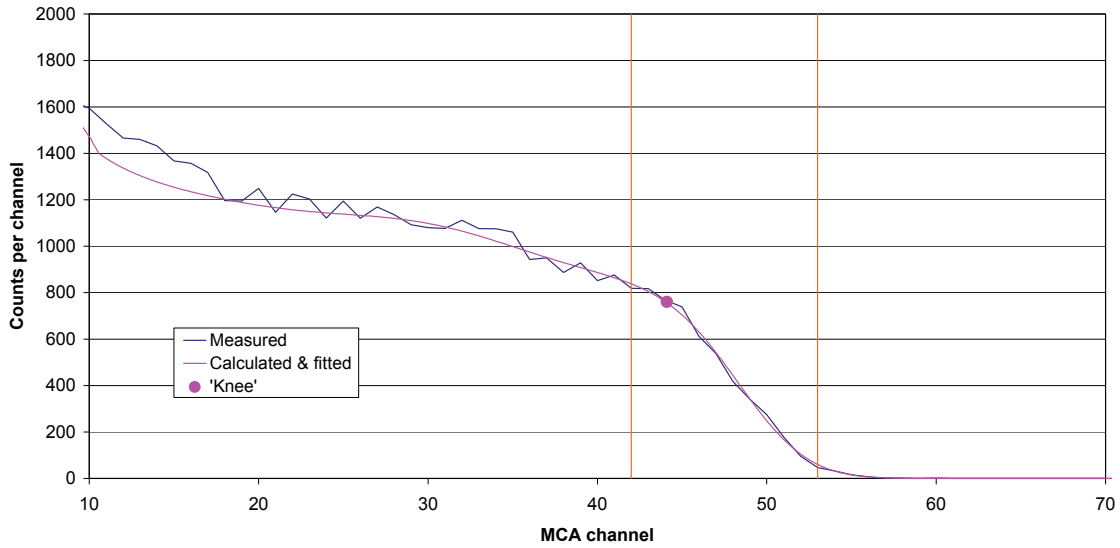

Figure 14. Typical outcome of the recoil edge fitting process in neutron spectra. The spectrum shown is that of the non-absolute 2.5 MeV measurement. Fitting was confined to the region between the vertical lines. The filled circle shows the assumed location of the 'knee' (the transition from the edge to the nominally flat top of the recoil distribution), and the half-height position follows as the channel number (non-integral in general) at which the spectrum height falls to half its value at the knee. The displacement factor determined in this way for this spectrum was $f = 1.001$, which supports the assumption in Reference 1 that f can be taken as equal to 1 for such spectra.

The light output calibration of each neutron spectrum was established by reference to ^{22}Na measurements, one for each experimental session. To determine the position of the ^{22}Na edge in these measured spectra, the calculated shape of the ^{22}Na Compton edge was scaled to match the data, and the half-height position was then easily established from the smooth calculated curve, without the distractions of channel-to-channel statistical fluctuations. This position was then associated with the known light output of the ^{22}Na upper edge half height, namely $f\,L_e(E_c(E_\gamma))$, with the same values as in Equation 5. In cases where the ^{22}Na source had been placed in front of the spectrometer for the calibration, the calculated spectrum used in this process was the one on which Figure 10 is based. In cases where the source had been placed on the side of the scintillator cell, a new calculation was carried out with side entry specified, although this change of geometry is not expected to have any great impact.

The proton light output function deduced from the neutron measurements is shown in Figures 15 and 16. The functional form chosen to fit the data was a power law in proton energy, joining smoothly onto a straight line, which is one of the forms available in NRESP7. The fit involved a total of three free parameters because the energy of the join was also adjustable. OriginPro[18] was again used for the fitting process.

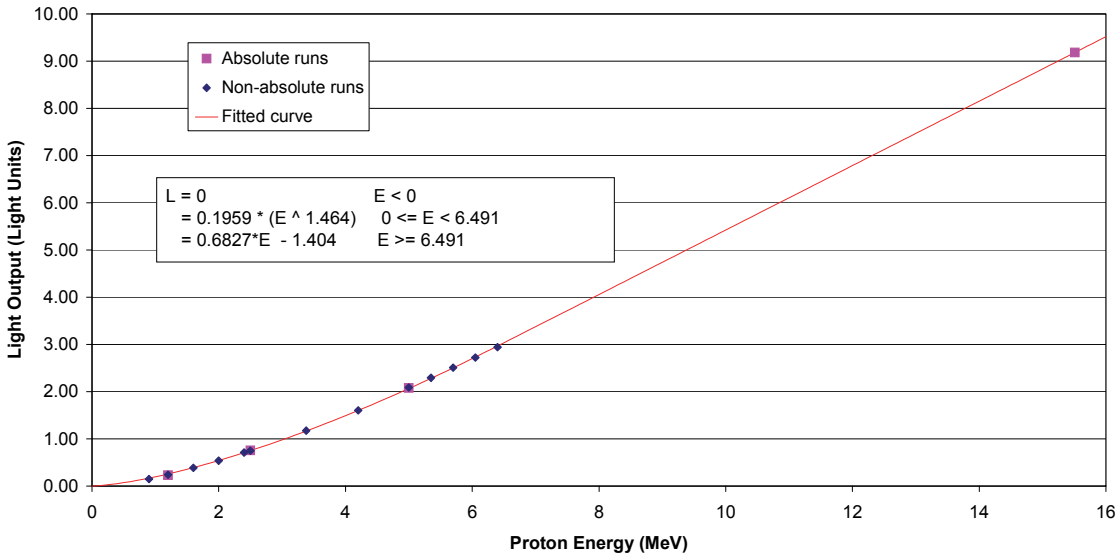

Figure 15. Proton light output function (showing full energy range).

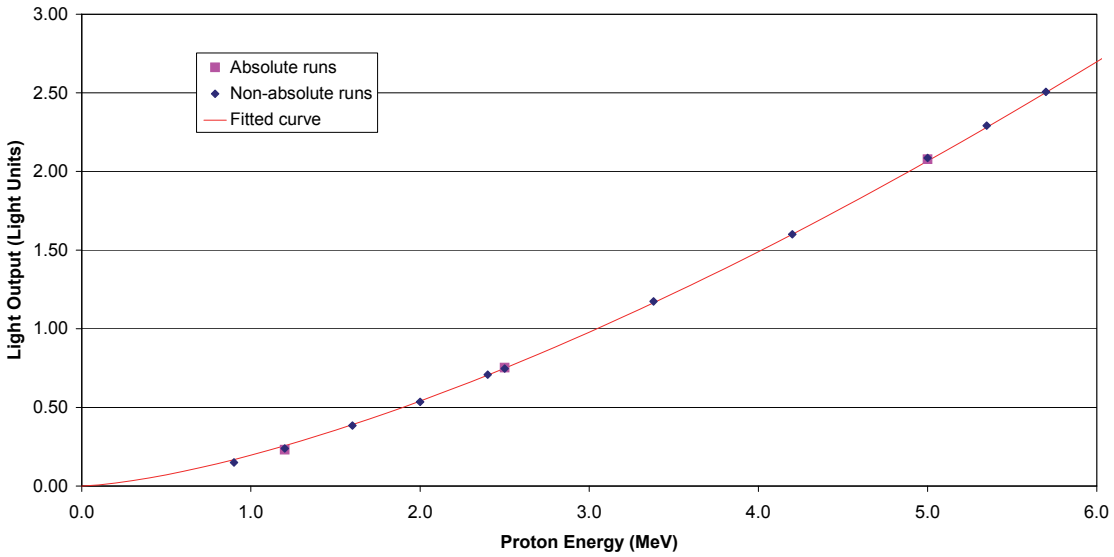

Figure 16. Proton light output function (showing low energies only).

The neutron resolution data, determined at the same time as the light output data in step (iv) above, were combined with the gamma resolution data as already described (Section 5.1.1) in order to obtain a fit to the combined data (Figure 7).

5.2.2 Comparison of calculated and measured neutron spectra

The proton light output function determined above was incorporated into NRESP7, and Gaussian smearing was specified using the light-dependent width already established, i.e.

$$\text{FWHM}\ (\%) = (A^2 + B^2/L + C^2/L^2)^{0.5}$$

with A = 8.550, B = 9.138 and C = 2.487 (Figure 7). New spectra were then calculated for each of the absolute measurements. The source distance used in each calculation was set equal to the distance in the corresponding measurement, and the source spectrum in the calculation was a rectangular distribution with full width calculated from the target properties. The energy parameters used in the calculations are listed in Table 4.

Comparisons between the measured and calculated pulse height spectra are given in Figures 17 - 20 below.

Table 4. Neutron energy parameters used in response calculations.

Neutron energy, MeV	Full width of energy distribution, MeV
15.51	0.620
4.985	0.129
2.500	0.028
1.201	0.040

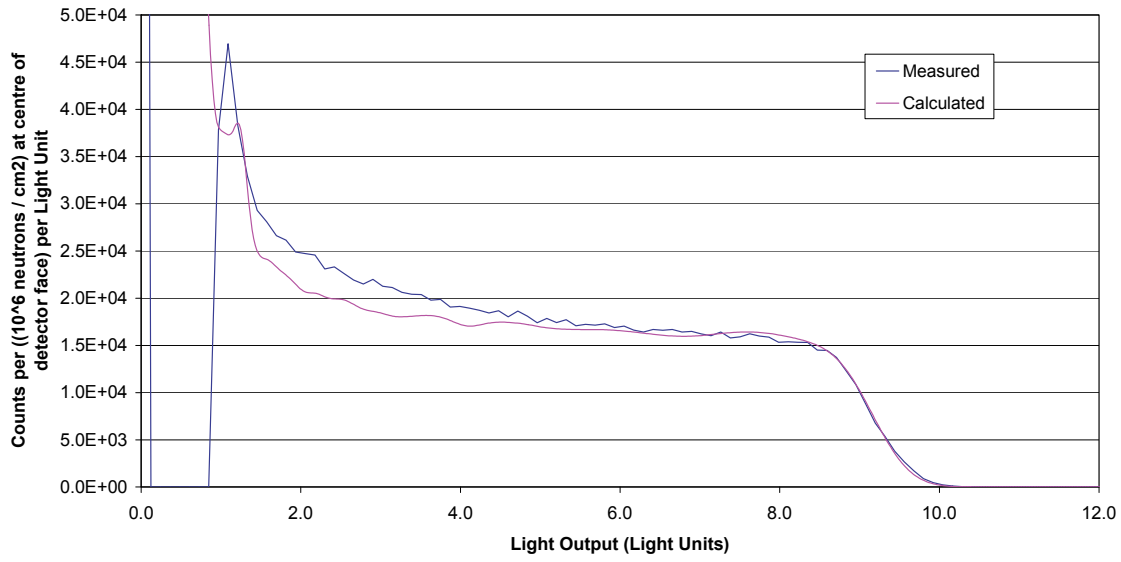

Figure 17. 15.5 MeV neutron response, measured and calculated.

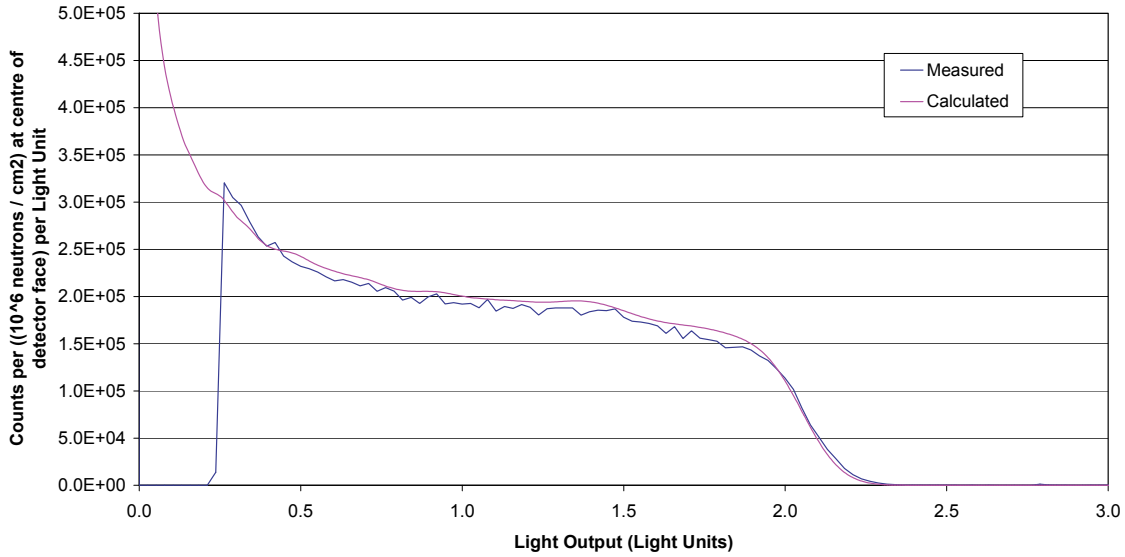

Figure 18. 5 MeV neutron response, measured and calculated.

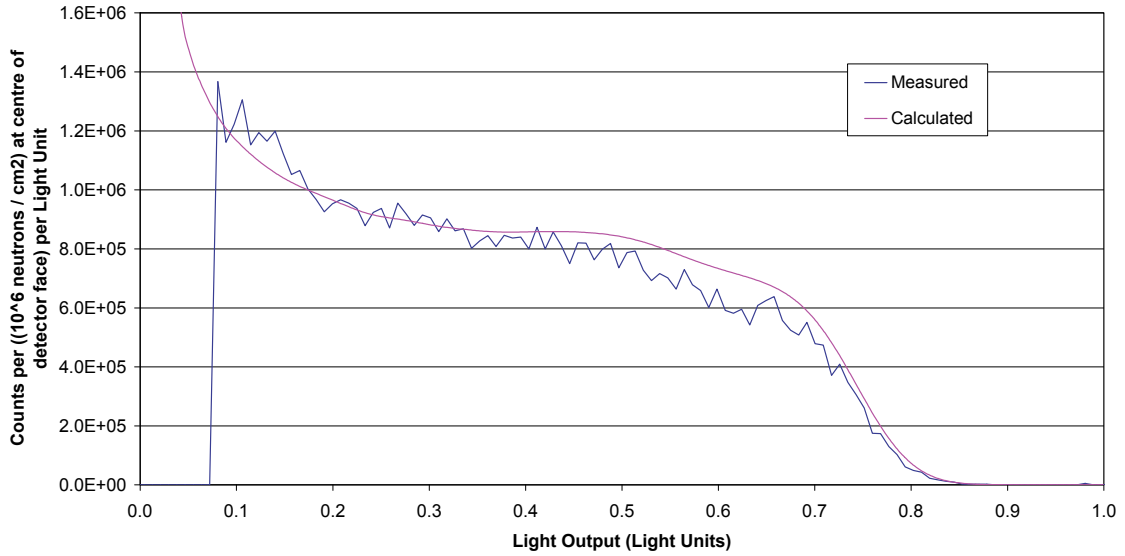

Figure 19. 2.5 MeV neutron response, measured and calculated.

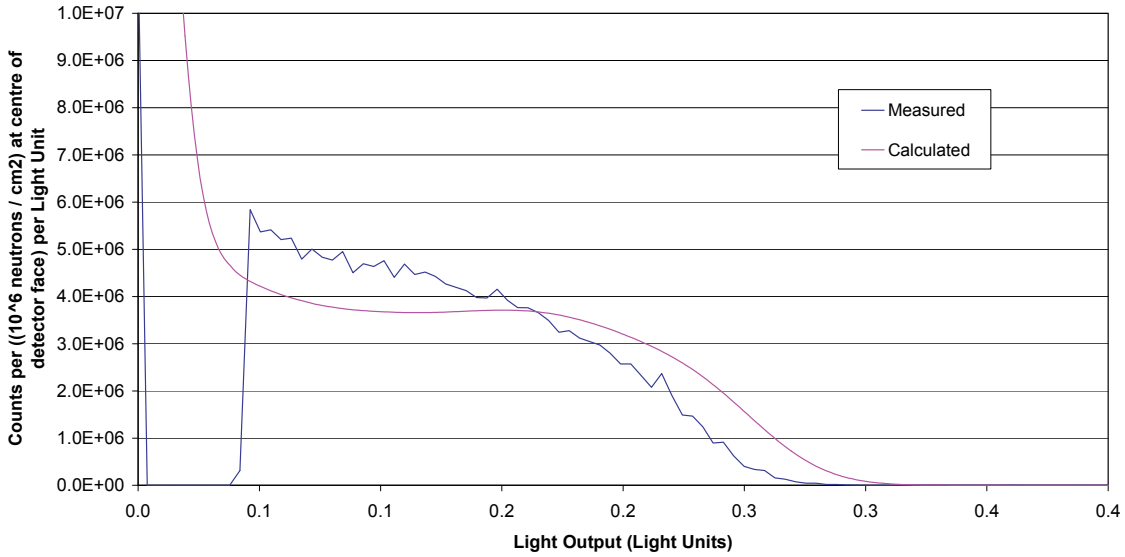

Figure 20. 1.2 MeV neutron response, measured and calculated.

As with the gamma calculations, both horizontal and vertical scales are absolute, except in so far as the experimental spectrum contributed to the light output function. The match between measurement and calculation is again reasonable to good, especially at the higher neutron energies. Within individual spectra, there is a tendency for the calculation to overestimate at the high proton energies and underestimate at the low (which is similar to the gamma case even though a different program is being used), and the explanation may be similar, namely some detector pulses may be being attenuated or the spectrometer may be producing low amplitude pulses by an unmodelled mechanism (including the possible production of low-energy neutrons from the target, particularly at 15 MeV). In the case of the 1.2 MeV spectrum, the discrepancy at high energies appears to be mainly due to imperfect modelling of the light output, as is just discernible in Figure 16.

NRESP7 was considered to have been validated for the Small spectrometer by this exercise, and the construction and use of a neutron response matrix is described below.

6 RESPONSE MATRICES AND SPECTRUM UNFOLDING

6.1 SMALL SPECTROMETER

6.1.1 Constructing a gamma response matrix

To generate a response matrix, a large number of response calculations are carried out at closely spaced energies, and the resulting pulse height spectra are assembled in the format appropriate for the unfolding program that is to be used.

To determine the energies at which to calculate the responses, the approach of the utility programs provided with PHRESP for this purpose was adopted. This approach is based on the principle that response functions are to be spaced most closely where the spectrometer resolution ΔL is smallest, and more widely where ΔL is larger. Roughly speaking, the method maintains the same number (7 in the present case) of response functions per light increment $\Delta L(L)$, where $\Delta L(L)$ is the absolute FWHM as derived from the formula in Figure 7, i.e., $\Delta L(L) = (A^2L^2 + B^2L + C^2)^{0.5}$ / 100 Light Units. For the Small spectrometer, a total of 199 response functions were calculated, covering gamma energies from 68.6 keV to 4949 keV, at intervals ranging from 4.6 keV to 66.9 keV.

For these calculations, the geometry of the model was altered to have a parallel gamma beam instead of a point source, as the distance to the source will not in general be known.

The calculated responses were assembled into the response matrix format required by the HEPROW package, using the utility programs BMATASC (which assembles a matrix with unsmeared response functions) and RSPGW (which adds smearing). These programs are part of the PHRESP and HEPROW packages.

6.1.2 Unfolding a gamma spectrum

To test this new response matrix, the experimental ^{24}Na spectrum measured with the Small spectrometer was unfolded using the HEPROW package.

The pulse height spectrum recorded over a 20 minute counting interval, with the ^{24}Na source at 4.15 cm from the front face of the spectrometer, is shown in Figure 21. A separate measurement with a ^{22}Na source was used to provide a light output calibration, in the same way as previously described for the neutron runs (Section 5.2.1). The program UMSPHW was used to convert the MCA data into a pulse height spectrum file in HEPROW format, and this was then passed to GRAVELW for unfolding, with a flat energy spectrum used as the starting point.

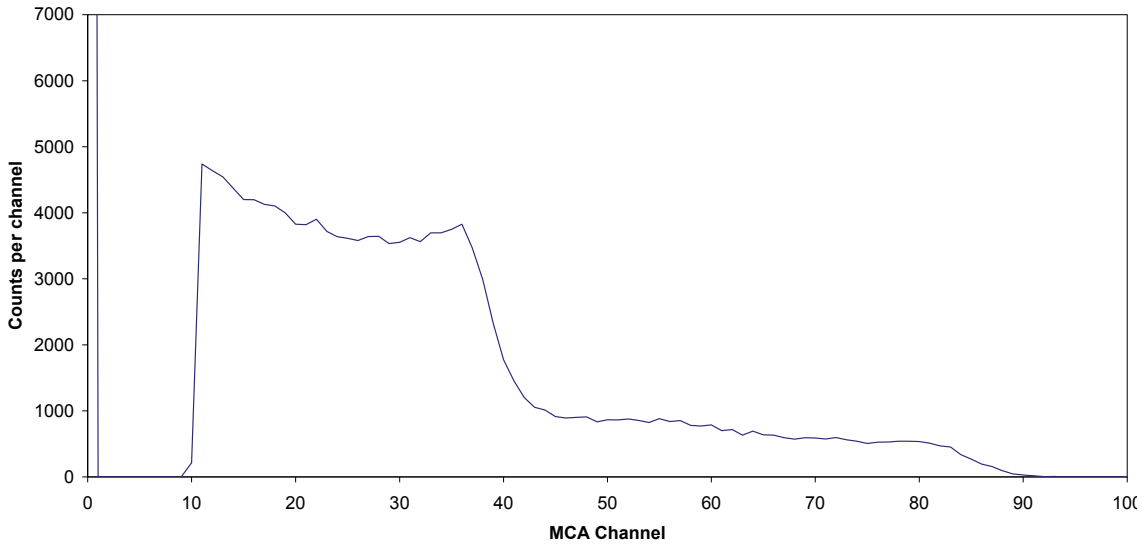

Figure 21. Measured pulse height spectrum for ^{24}Na source.

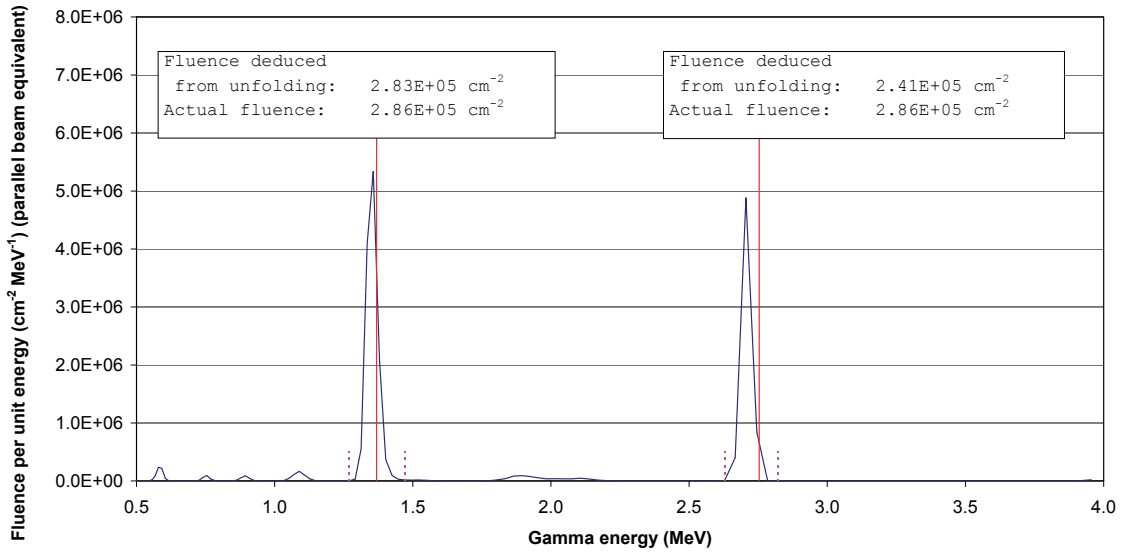

Figure 22. ^{24}Na gamma spectrum unfolded from measured data.
The vertical full lines show the actual gamma energies produced by the source. The text in the Figure compares the parallel-beam gamma fluence deduced from the unfolded spectrum (by integrating the peaks) with the actual fluence at the position of the centre of the scintillator (calculated from the source activity and distance). The short dotted lines show the bounds of the integrals.

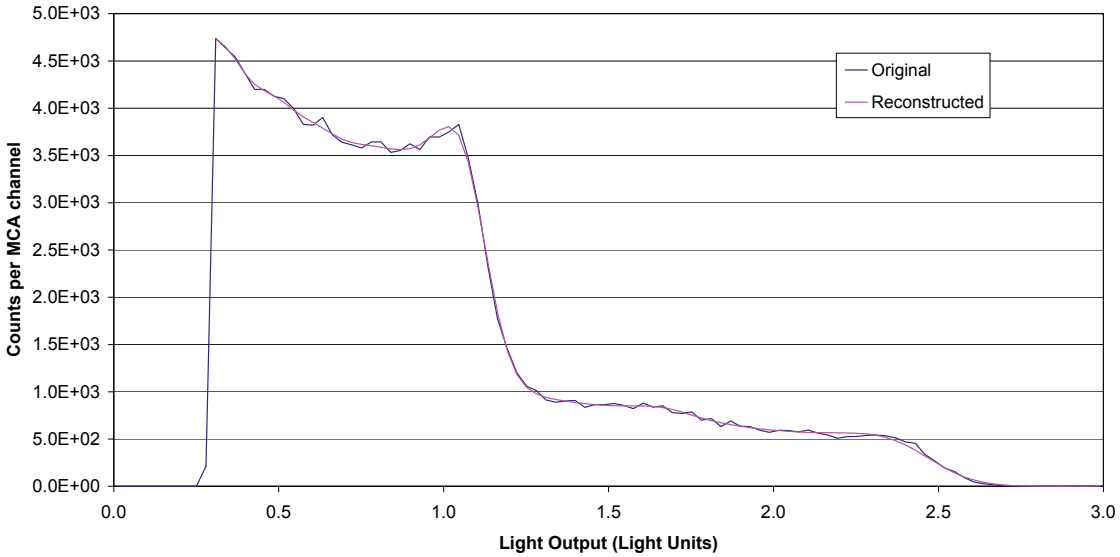

Figure 23. Reconstructed pulse height spectrum compared with original.
Purple line: result of folding the response matrix back into the fluence spectrum from the previous Figure. Blue line: original pulse height spectrum. (Here bins are labelled with the light output at the left hand side of the bin, according to HEPROW convention.)

The unfolded gamma energy spectrum is shown in Figure 22. It consists of two isolated sharp peaks, as expected, and the positions of the peaks agree to approximately 2% or better with the known gamma energies from the source. The fluences deduced from the areas of the peaks are also given in the Figure, and compared with the fluences calculated from the activity and distance of the source, the latter values being quoted at the position of the centre of the scintillator (in the absence of the spectrometer).

For the lower energy peak, the two fluence values agree well, although it must be remembered that the value from the unfolding is in terms of an equivalent parallel-beam fluence, because this is how the response matrix was constructed. From the geometry of the measurement, one would expect the parallel-beam fluence to exceed the actual fluence at the position of the centre of the scintillator by about 4%, so the figure derived from the unfolding is actually about 5% lower than expected.

For the higher energy peak, the fluence discrepancy is considerably larger, at about 20% in total. This does not appear to be due to a problem with the unfolding, because folding the spectrometer response back into the gamma spectrum produces a pulse height spectrum that agrees well with the measured data (Figure 23). It is possible that counts were lost from the measured pulse height spectrum because of the gamma acquisition problem detailed in Reference 1. (The Shape signal from gamma events can be very small, and this can cause the acquisition system to discard the event.) Figure 24 shows the 2-parameter data corresponding to the ^{24}Na measurement, and is apparent that the high-energy end of the distribution may have been affected.

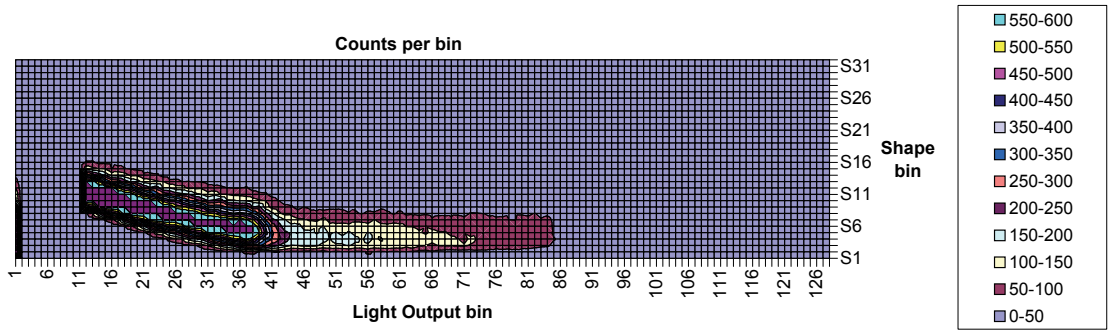

Figure 24. Two-parameter data from the ^{24}Na measurement with the Small spectrometer. (The purple colour denotes bins with more than 600 counts.) Possible distortion of the upper end of the pulse height spectrum is evident.

6.1.3 Constructing a neutron response matrix

The neutron response matrix was assembled in a similar way to that for gammas. The NRESP7 calculation was set up for a distant (10 m) source as an approximation to a parallel beam, and the energies for the response calculations were again chosen so as to hold the number of response functions per resolution width ΔL approximately constant (at 4 this time). 129 response functions were calculated, at energies from 0.393 MeV to 12.186 MeV, with intervals varying from 41.5 keV to 229 keV. Two utility programs written previously for the Large spectrometer were used in the creation of the response matrix, one to generate the large number of NRESP7 input lines needed to calculate all the responses, and the other to assemble those responses into a matrix in HEPROW format.

6.2 LARGE SPECTROMETER

6.2.1 Unfolding a gamma spectrum

The unfolding of a ^{24}Na pulse height spectrum measured with the Large spectrometer, using a response matrix constructed for that spectrometer, was reported in Reference 1. It was noted that the widths of the unfolded peaks were unexpectedly large.

It has since been established that the smearing parameters used by the program RSPGW to add Gaussian smearing to the responses in the matrix actually describe the FWHM of the Gaussian and not the standard deviation as believed at the time. The responses in the original matrix were therefore too narrow, and the unfolded peaks too wide.

This problem has now been rectified, and the revised unfolded gamma spectrum is shown in Figure 25.

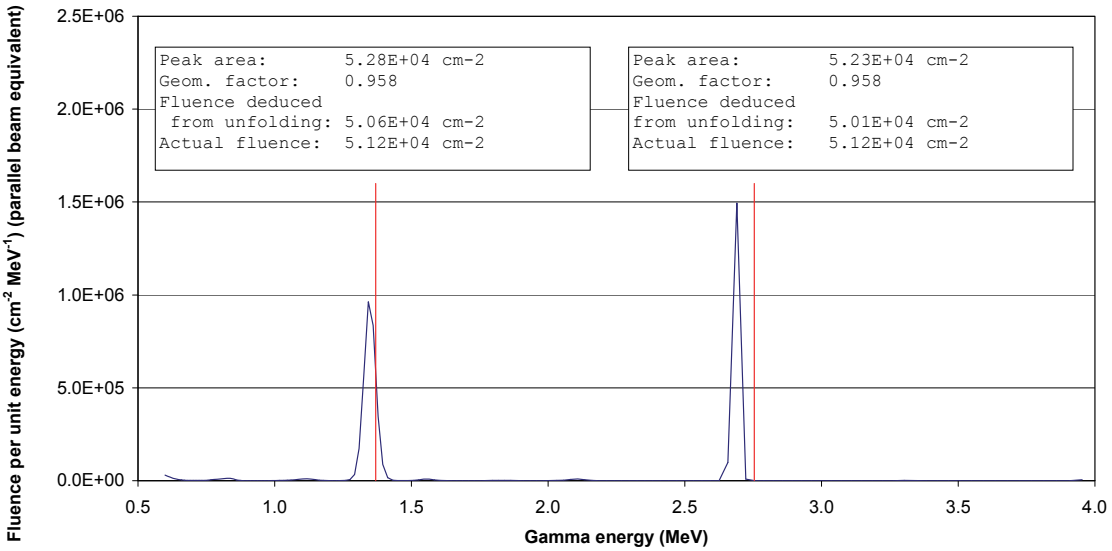

Figure 25. ^{24}Na spectrum unfolded from data measured with the Large spectrometer. The vertical lines show the actual gamma energies produced by the source. The text compares the fluence deduced from the unfolding with the fluence calculated from the source activity and distance, both values being quoted at the position of the centre of the scintillator.

The revised spectrum displays a much reduced width in both peaks. The positions of the peaks remain close to the known energies of the gamma rays (although the upper peak appears slightly low, as is also the case for the Small spectrometer). For this measurement a geometry factor, calculated using additional PHRESP runs, is available to relate the parallel-beam fluence to the fluence at the position of the centre of the scintillator, and the text in Figure 25 shows how this compares with the corresponding fluence calculated from the source activity and distance. Agreement is good, not just for the lower peak but the upper as well. It is interesting that, with the Large spectrometer, the 2-parameter data for this measurement (Figure 26) do not show the potential problem at high energies that affected the Small spectrometer (Figure 24).

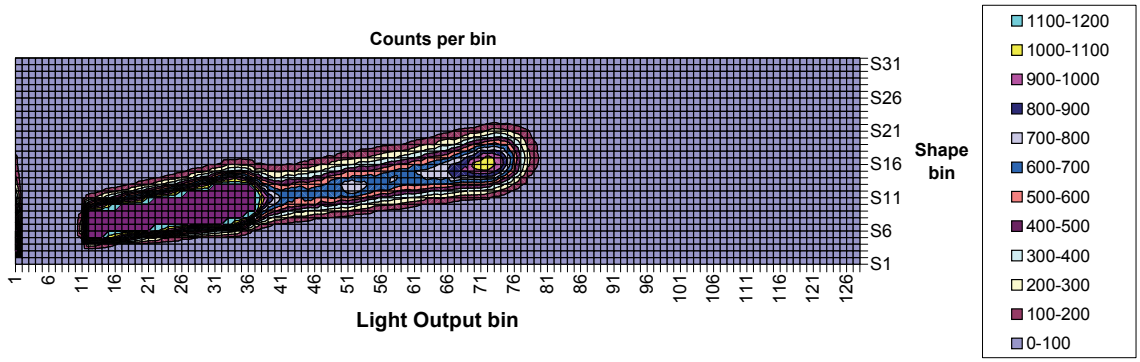

Figure 26. 2-parameter data from the ^{24}Na measurement with the Large spectrometer. (The purple colour denotes bins with more than 1200 counts.) The trend of the Shape signal is opposite to that seen with the Small spectrometer, and the gamma event distribution remains well clear of the lower Shape bound.

6.2.2 Unfolding a neutron spectrum

In Reference 1, the construction of a neutron response matrix for the Large spectrometer was reported, but no neutron spectrum was unfolded. A neutron spectrum from a ^{241}Am / Be neutron source has now been measured and the result compared with the corresponding spectrum given in ISO 8529-1:2000[20].

The measurement was made over 6730 s of live time with a 555 GBq (15 Ci) ^{241}Am / Be source at 292.4 cm from the front face of the Large spectrometer. A shadow cone run was carried out to allow room scatter to be subtracted, and a separate measurement with a ^{22}Na source was made in order to provide a light output scale.

The measured neutron pulse height spectrum is shown in Figure 27. Room scatter has been subtracted, and the gamma contribution from the source has been removed as described in Section 4.2.1.

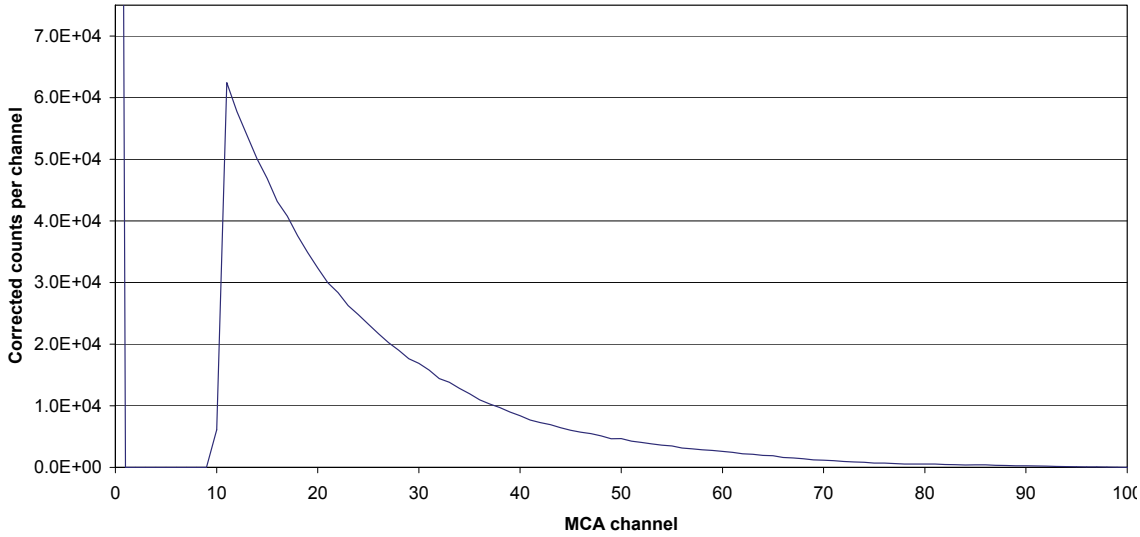

Figure 27. Neutron pulse height spectrum from an NPL ^{241}Am / Be source. Room scatter and the gamma contribution have both been subtracted.

The pulse height spectrum was associated with a light output scale using the ^{22}Na calibration, converted to HEPROW format, and passed to GRAVELW for unfolding. The result is shown in Figure 28.

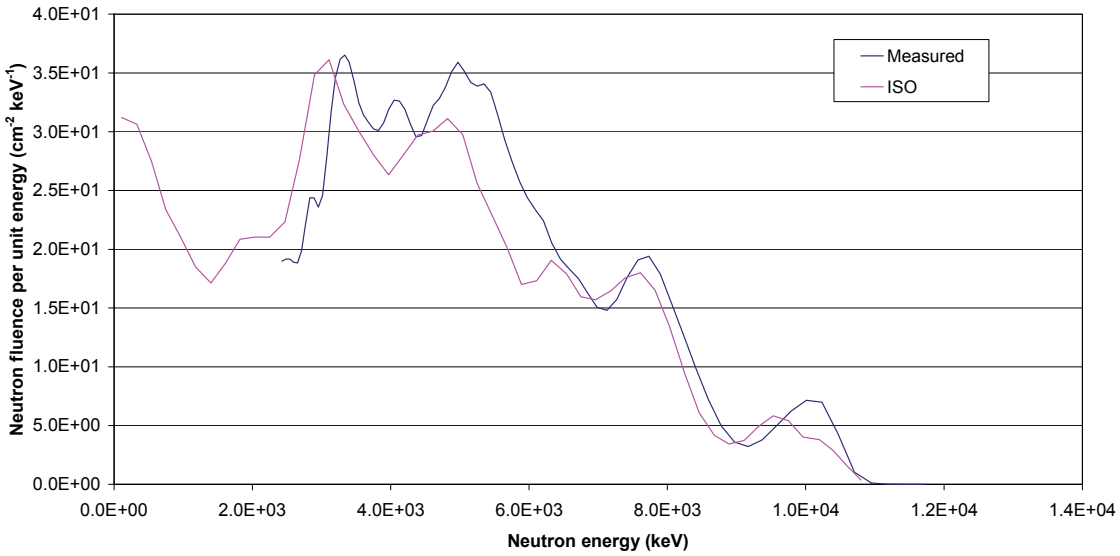

Figure 28. Measured ^{241}Am / Be spectrum compared with ISO spectrum.

The horizontal and vertical scales in Figure 28 are both absolute, the energy scale for the measured spectrum having been established by the ^{22}Na calibration, and the vertical scale for the ISO spectrum being based on the known fluence from the NPL source at the distance of the centre of the scintillator. Despite the absence of any obvious features in the pulse height spectrum, the unfolded energy spectrum appears to reproduce the main aspects of the ISO spectrum, in both energy and amplitude (except possibly in the region of 6000 keV, where there is a noticeable energy difference).

7 CONCLUSIONS

The characterisation carried out previously for the Large spectrometer has now been repeated for the Small, and electron, proton and resolution functions are now known for both spectrometers. A new neutron response matrix has been constructed, and a gamma matrix constructed for the first time, for the Small spectrometer, and a corrected gamma response matrix has been produced for the Large spectrometer. Both types of matrix are therefore available, in HEPROW format, for both spectrometers.

Both spectrometers have successfully produced unfolded gamma spectra from a ^{24}Na source, and the Large spectrometer has produced an unfolded ^{241}Am / Be neutron spectrum that is a good match to the ISO spectrum for the same type of source.

8 ACKNOWLEDGEMENTS

Thanks are due to Neil Roberts for making available his calculations of the neutron fluence per monitor count at PTB, and to David Thomas for his helpful comments on the manuscript. Financial support from the National Measurement Office, an executive agency of the UK Government's Department for Business, Innovation & Skills, is gratefully acknowledged.

9 REFERENCES

1. HAWKES, N.P. and ASHLEY, S.F. Progress in characterising the neutron and gamma responses of the NPL liquid scintillation spectrometers, *NPL Report IR 9*, May 2008.
2. Saint-Gobain Crystals, www.detectors.saint-gobain.com
3. GREEN, S., SCOTT, M. and KOOHI-FAYEGH, R. *A users' guide for the NPL NE-213 Neutron Spectrometry System*, School of Physics and Space Research, University of Birmingham, September 1991, unpublished.
4. OWEN, R.B. *Nucleonics,* 1959, **17,** 92.
5. MCCRACKEN, A.K. and GRIMSTONE, M.J. The experimental data processing program RADAK, *Proceedings of the First ASTM Symposium on Reactor Dosimetry*, Petten, 1975.
6. TEXTOR, R.E. and VERBINSKI, V.V. O5S: a Monte-Carlo code for calculating the pulse height distributions due to monoenergetic neutrons on organic scintillators, *Oak Ridge National Laboratory Report ORNL-4160*, 1968.
7. ADAMS, J.M., WATKINS, N., KLEIN, H. and LEBRETON, L. Private communications, 2003 – 2004.
8. NOVOTNY, T. Photon spectrometry in mixed neutron-photon fields using NE213 liquid scintillation detectors, *PTB Report PTB-N-28*, 1997.
9. DIETZE, G. and KLEIN, H. NRESP4 and NEFF4: Monte Carlo codes for the calculation of neutron response functions and detection efficiencies for NE213 scintillation detectors, *PTB Report PTB-ND-22*, October 1982 (with supplement for version 7, August 1991).
10. MATZKE, M. Unfolding of pulse height spectra: the HEPRO program system, *PTB Report PTB-N-19*, 1994. (See also HEPROW.pdf, available from http://www.matzke-bs.de/heprow/heprow.htm.)
11. DIETZE, G. and KLEIN, H. Gamma-calibration of NE213 scintillation counters, *Nucl. Instrum. Methods*, 1982, **193**, 549 - 556.
12. NOVOTNY, T., BÜERMANN, L., GULDBAKKE, S. and KLEIN, H. Response of NE213 liquid scintillation detectors to high-energy photons (7 MeV < E_γ < 20 MeV), *Nucl. Instrum. Methods in Phys. Res.*, 1997, **A400**, 356 - 366.
13. HAWKES, N.P., ADAMS, J.M., BOND, D.S., CROFT, S., JARVIS, O.N. and WATKINS, N. Measurements of the Proton Light Output Function of the Organic Liquid Scintillator NE213 in Several Detectors, *Nucl. Instrum. Methods in Phys. Res.*, 2002, **A476**, 190-194.
14. http://www.hightechsource.co.uk
15. http://www3.imperial.ac.uk/reactorcentre
16. DIETZE, G. Energy calibration of NE213 scintillation counters by γ-rays, *IEEE Transactions on Nuclear Science*, 1979, **NS-26**, 398 – 402.
17. KLEIN, H. and NEUMANN, S. Neutron and photon spectrometry with liquid scintillation detectors in mixed fields, *Nucl. Instrum. Methods in Phys. Res.*, 2002, **A476**, 132 – 142.
18. See web site http://www.originlab.com/
19. See web site http://www.nucleide.org/DDEP_WG/DDEPdata.htm
20. International standard ISO 8529-1, *Reference neutron radiations -- Part 1: Characteristics and methods of production*, International Organization for Standardization, http://www.iso.org/iso/home.htm.